Title

Measurement Floors and Dynamic Ranges of OCT and OCT Angiography in Glaucoma

Journal

Ophthalmology, 126(7)

ISSN

0161-6420

Authors

Moghimi, Sasan
Bowd, Christopher
Zangwill, Linda M
et al.

Publication Date

2019-07-01

DOI

10.1016/j.ophtha.2019.03.003

Peer reviewed

HHS Public Access

Author manuscript

Ophthalmology. Author manuscript; available in PMC 2020 July 01.

Published in final edited form as:

Ophthalmology. 2019 July ; 126(7): 980–988. doi:10.1016/j.ophtha.2019.03.003.

Measurement floors and dynamic ranges of optical coherence tomography and angiography in glaucoma

Sasan Moghimi, MD[1], **Christopher Bowd, PhD**[1], **Linda M. Zangwill, PhD**[1], **Rafaella C. Penteado, MD**[1], **Kyle Hasenstab, PhD**[1], **Huiyuan Hou, MD, PhD**[1], **Elham Ghahari, MD**[1], **Patricia Isabel C. Manalastas, MD**[1], **James Proudfoot, MSc**[1], and **Robert N. Weinreb, MD**[1,*]

[1]Hamilton Glaucoma Center, Shiley Eye Institute, Viterbi Family Department of Ophthalmology, University of California, San Diego, CA, United States.

Abstract

Purpose: To determine if optical coherence tomography angiography (OCTA)-derived vessel density measurements can extend the available dynamic range for detecting glaucoma compared to spectral-domain optical coherence tomography (SDOCT)-derived thickness measurements.

Design: Observational, cross-sectional study.

Participants: A total of 509 eyes from 38 healthy participants, 63 glaucoma suspects and 193 glaucoma patients enrolled in the Diagnostic Innovations in Glaucoma Study.

Methods: Relative vessel density and tissue thickness measurement floors of perifoveal superficial vessel density (pfVD), circumpapillary capillary density (cpCD), circumpapillary retinal nerve fiber (cpRNFL) thickness, ganglion cell complex (GCC) thickness and visual field mean deviation were investigated and compared with a previously reported linear change point model (CPM) and locally weighted scatterplot smoothing (LOWESS) curves.

Main Outcome Measures: Estimated vessel density and tissue thickness measurement floors and corresponding dynamic ranges.

Results: Visual field MD ranged from −30.1 dB to 2.8 dB. No measurement floor was found for pfVD which continued to decrease constantly until very advanced disease. A true floor (i.e. slope ~ 0 after observed CPM change point) was detected for cpRNFL thickness only. Post-CPM estimated floors were 49.5±2.6 μm for cpRNFL thickness, 70.7±1.0 μm for GCC thickness and 31.2± 1.1% for cpCD. pfVD reached the post-CPM estimated floor later in the disease (VF MD: −25.8±3.8 dB) than cpCD (VF MD: −19.3±2.4 dB), cpRNFL thickness (VF MD: −17±3.3 dB) and GCC thickness (VF MD: −13.9±1.8 dB) ($p<0.001$). The number of available measurement

[*]**Corresponding author:** Robert N. Weinreb, University of California San Diego, La Jolla, California, rweinreb@ucsd.edu.

The following authors have no financial disclosures: Sasan Moghimi, Christopher Bowd, Kyle Hasenstab , Rafaella C. Penteado, Huiyuan Hou, Elham Ghahari, Patricia Isabel C. Manalastas, and James Proudfoot. All authors attest that they meet the current ICMJE criteria for authorship.

steps from normal values to the CPM estimated floor was greatest for cpRNFL thickness (8.9), followed by GCC thickness (7.4), cpCD (4.5) and pfVD (3.8).

Conclusion: In late-stage glaucoma, particularly when VF MD is worse than −14 dB, OCTA-measured pfVD is a promising tool for monitoring progression as it does not have a detectable measurement floor. However, the number of steps within the dynamic range of a parameter also needs to be considered. Although thickness parameters reached the floor earlier than OCTA-measured pfVD, there are more such steps with thickness than OCTA parameters.

Précis:

A measurement floor is not detected with optical coherence tomography angiography in advanced glaucoma. OCT-A -measured vessel density may be useful for monitoring such patients for progression.

Keywords

optical coherence tomography angiography; Glaucoma; optical coherence tomography; Retinal nerve fiber layer

Introduction

Primary open angle glaucoma (POAG) is an optic neuropathy characterized by progressive loss of retinal ganglion cells and their axons and an accompanying decrease in visual field (VF) sensitivity.[1, 2] Detecting disease progression is essential for determining whether a patient is stable and current treatment is effective or if the patient is progressing and treatment must be modified. Determination of progression is particularly important in advanced glaucoma patients who are at the greatest risk of becoming functionally impaired or blind from the disease.[3]

Spectral domain optical coherence tomography (SDOCT) allows quantitative assessment of circumpapillary retinal nerve fiber layer (cpRNFL) thickness and ganglion cell complex (GCC) thickness with excellent reproducibility.[4–6] Changes in these structures over time have been shown to be reliable indices of glaucoma progression that may detect glaucomatous change earlier than VF testing.[7, 8] However, detection of glaucomatous change in advanced POAG is challenging because of the existence of a “floor effect” after which no further structural change can be detected in OCT-based cpRNFL thickness measurements and an increase in variability of VF measurements.[9–12] Regardless of the specific OCT instrument used to acquire the measurements, reported cpRNFL thicknesses rarely are lower than 45 to 55 μm, even in end-stage disease.[12, 13] However, some recent studies indicate that ganglion cell-inner plexiform layer (GCIPL) thickness is less likely to reach a measurement floor in advanced disease than cpRNFL thickness suggesting the GCIPL thickness may a better metric than RNFL thickness for detecting progression in late stages.[13–15]

Optical coherence tomography angiography (OCTA) noninvasively images the blood vessels of the ONH and retina in vivo[16] and offers the potential for enhancing our understanding of the role of ocular blood flow and the retinal microvasculature in glaucoma.[17, 18] Vessel

density measurements provided by OCTA are repeatable and reproducible.[6, 19] A reduction in vessel density surrounding the optic nerve head and macula has been demonstrated in glaucomatous compared to healthy eyes.[18, 20–24] A recent study reported that superficial macula vessel density change is detectable using OCTA after a short follow-up of 13 months and prior to significant thinning of the GCC in some eyes.[25] To our knowledge, there has not been any report of floor effects for OCTA vessel density measurements to date.

Identification of VF sensitivity at the measurement floors for OCTA vessel densities and comparisons with similar SDOCT thickness measurements can provide information applicable to the relative utility of OCTA and SDOCT parameters for measuring glaucomatous progression. Moreover, additional information can be gained by determination of both the dynamic range (in relation to measurements from healthy eyes) and the average number of measurable steps between healthy measurements and the measurement floor (as a function of test-retest variability in glaucoma eyes). The latter metric has particular clinical importance because more measurable steps provide more opportunities to detect a significant change before a given parameter reaches its measurement floor.[12, 13, 26]

If OCTA-measured vessel density parameters reach a measurement floor further along the disease severity continuum than OCT-measured thickness parameters, vessel density parameters may be relatively more useful for assessing structural progression in advanced glaucoma. The current study investigated vessel density-function and RNFL and GCC thickness-function relationships measured using OCTA, SDOCT and automated perimetry VF measurements. Further, it compared the dynamic ranges of vessel density and thickness parameters to estimate the VF mean deviation (MD) at which these parameters reach their respective measurement floors.

Methods

Participants from the Diagnostic Innovations in Glaucoma Study (DIGS) who underwent OCTA, SDOCT imaging and visual field testing were included in this cross-sectional study. The Institutional Review Board of the University of California San Diego approved the protocol, and the methodology adheres to the tenets of the Declaration of Helsinki for research involving human subjects and to the Health Insurance Portability and Accountability Act. Informed consent was obtained from all participants.

The DIGS protocol and eligibility criteria have been described in detail previously.[27] In brief, all participants underwent an ophthalmologic examination, including assessment of best-corrected visual acuity, slit-lamp biomicroscopy, intraocular pressure (IOP) measurement with Goldmann applanation tonometry, gonioscopy, ultrasound pachymetry, dilated fundus examination, simultaneous stereophotography of the optic disc, and visual field testing (standard automated perimetry; Humphrey Field Analyzer II with 24–2 Swedish Interactive Thresholding Algorithm; Carl Zeiss Meditec, Fremont, CA). Eligible participants had a best-corrected visual acuity of 20/40 or better, spherical refraction within ±5.0 diopters, cylinder correction within ±3.0 diopters.

Eyes with a history of intraocular surgery (except uncomplicated cataract surgery or uncomplicated glaucoma surgery), coexisting retinal pathology, non-glaucomatous optic neuropathy, uveitis, or ocular trauma were excluded for the study as were individuals with a diagnosis of Parkinson's disease, Alzheimer's disease, dementia, a history of stroke, or with diabetic or hypertensive retinopathy. DIGS protocol requires images be obtained at least 3 months after cataract or glaucoma surgery. Eyes included in the current study all were imaged no less than 6 months after either procedure.

Measurements from healthy, glaucoma suspect and glaucoma eyes (defined below) were included to represent the disease severity continuum from healthy to advanced glaucoma. Healthy eyes were defined as having a healthy appearance of the optic nerve and parapapillary retina by masked stereoscopic optic disc photograph assessment, intraocular pressure (IOP) less than 22 mmHg, no history of elevated IOP, and at least 2 reliable (fixation losses and false-negatives ≤ 33% and false-positives ≤ 15%) normal VF results, defined as a pattern standard deviation (PSD) within 95% confidence limits and Glaucoma Hemifield Test (GHT) results within normal limits.

Glaucoma suspects were defined as having glaucomatous optic neuropathy on stereophotograph assessment and/or ocular hypertension (IOP ≥ 22 mm Hg) without evidence of repeatable glaucomatous VF damage.

Glaucomatous eyes were defined as having glaucomatous optic neuropathy by stereoscopic photograph assessment (i.e., the presence of focal or diffuse narrowing of the neuroretinal rim or localized or diffuse atrophy of the RNFL) and repeatable and reliable abnormal VFs outside of attributable to glaucoma. Outside of normal limits was defined as a PSD ≥ 95% or a GHT result outside of normal limits. VFs were visually assessed to confirm that patterns of defect in consecutive abnormal fields were similar. Mild to moderate glaucoma was defined as VF MD higher than −12 decibels (dB), and advanced glaucoma was defined as a VF MD lower than −12 dB. Systemic blood pressure (BP) was measured in a seated position using the Omron Automatic (Model BP791IT; Omron Healthcare, Inc., Lake Forest, IL, USA) blood pressure monitor. Mean arterial pressure was calculated as one-third systolic BP + two-thirds diastolic BP. Mean ocular perfusion pressure (MOPP) was defined as the difference between two-thirds of mean arterial pressure and IOP.

Optical Coherence Tomography Angiography

The OCT AngioVue system (Optovue Inc., Fremont, CA, USA) incorporated in the Avanti SDOCT system was used for characterizing the vascular structures of the retina at the capillary level (using software version 2017 1.0.144). This system has been described previously.[16] The split-spectrum amplitude-decorrelation angiography (SSADA) method was used to capture the dynamic motion of the red blood cells and provide a high-resolution 3D visualization of perfused retinal vasculature.[28] Vessel density (defined as the percentage of a selected image area occupied by flowing vessels) within the RNFL was measured from the internal limiting membrane (ILM) to RNFL posterior boundary after removal of large vessels (called circumpapillary capillary density, cpCD). For this study, peripapillary vessel density was derived from the images acquired with a 4.5 X 4.5 mm^2 (304X304 A-scans) field of view centered on the optic disc. Macular vessel density measurements were

calculated from 3 × 3 mm^2 scans (304×304 A-scans) centered on the fovea. cpCD was calculated in the region defined by a 750μm-wide elliptical annulus extending from the optic disc boundary. Macular superficial vessel density measurements were calculated in a slab from the ILM to the posterior border of the inner plexiform layer (IPL). Perifoveal vessel density (pfVD) was measured in an annular region with an inner diameter of 1 mm and outer diameter of 2.5 mm in the superficial layer. Experienced reviewers masked to participants' clinical information reviewed OCTA image quality. Optic disc boundary placement and tissue segmentation were corrected manually as necessary. Poor quality Images were identified based on the UC San Diego Imaging Data Evaluation and Analysis (IDEA) Center protocol as images with (1) a signal quality index (SQI) of less than 4, (2) poor clarity, (3) motion artifacts visible as irregular vessel patterns, vessel doubling, or disc boundaries on the enface angiogram, (4) local weak signal, or (5) segmentation errors that could not be corrected manually, and were excluded. All images of borderline quality or excluded due to poor quality other than poor SQI, and a sample of acceptable quality scans were reviewed by at least 2 graders to ensure consistency of grading.

Spectral-Domain Optical Coherence Tomography

The Spectralis SDOCT (Spectralis HRA+OCT; Heidelberg Engineering Inc., Heidelberg, Germany) was used to measure circumpapillary RNFL thickness (software version 5.4.7.0). Spectralis OCT uses a dual-beam SDOCT, a confocal laser-scanning ophthalmoscope with a wavelength of 870 nm, and an infrared reference image to obtain images of ocular microstructures. Spectralis OCT has an acquisition rate of 40,000 A-scans per second and incorporates a real-time eye-tracking system that couples confocal laser-scanning ophthalmoscopy and SDOCT scanners to adjust for eye movements. The cpRNFL thickness was measured using the high-resolution RNFL circle scan, which is a single 12-degree b-scan circle centered on the optic disc composed of 1536 A-scans. Images with poor centering, inaccurate segmentation of the cpRNFL or quality scores of 15 dB or less were excluded from the analysis.

The Avanti (Optovue Inc.) macula cube scanning protocol was used to measure the macular ganglion cell complex (GCC) thickness. The GCC scanning protocol consists of a 7×7 mm^2 raster scan consisting of 1 horizontal B scan of 933 A-scans and 15 vertical B scans of 933 A-scans per B-scan. This protocol measures retinal thickness from the ILM to the IPL posterior boundary. Macular GCC thickness measurements are composed of the ganglion cell layer, inner plexiform layer and the RNFL. Acceptable-quality images were defined as scans with a signal strength index ≥ 48 without segmentation failure or artifacts (missing or blank areas).

Statistical Analyses

Statistical analyses were performed using STATA v. 15.0 (StataCorp, College Station, TX) and R version 3.3.1 (http://www.r-proiect.org). Statistical significance for tests was set at $P \leq 0.05$. Distribution of the numerical variables was explored with histograms. Analysis of variance (ANOVA) and post-hoc Tukey's Honestly Significant Difference (HSD) tests were calculated to compare demographic numeric parameters among healthy, glaucoma suspect

and glaucoma groups. Mixed effects modeling was used to compare ocular parameters among groups while accounting for correlations between the two eyes.

Vessel density-function and thickness-function relationships were investigated using two methods:

1) The first method, change point method (CPM), enables flexible linear relationships between anatomical measurements and visual function by allowing differing slopes before and after the change point. CPM is a derivation of the change point of the simple linear regression relationship between cpRNFL thickness and visual function previously described.29 The slopes (and 95% confidence intervals) before and after change points were calculated and compared for each vessel density or thickness parameter as follows:

$$Y = b + \alpha(x) + \mathscr{E} \text{ if } x < C$$

$$y = b + \alpha(x) + \beta(x - C) + \mathscr{E} \text{ if } x \geq C$$

Where b is the intercept in % or μm, α is the slope of the plateau portion (in %/dB or μm/dB), β is the difference between the slope of the steep and plateau portions (in %/dB or μm/dB), and C is the VF MD at the point of change intersection of two slopes). Hence, the slope of the steep portion was calculated as β + α.

Due to the inter-individual variability in vessel density and thickness measurements, we calculated the post-change point floor by averaging all thickness or density measurements at or after the calculated change point, similar to methods described by Mwanza et al.12 The corresponding VF MDs for the estimated floors in the fitted model were reported.

2) Locally weighted scatterplot smoothing (LOWESS) curves also were used to fit the relationships graphically. LOWESS is a modeling method that combines linear least squares regression with nonlinear regression30 by fitting simple models to localized subsets of the data to build a function that describes the deterministic part of the variation in the data, point by point. The LOWESS curve has the advantage of describing the structure-function relationship that is not constrained by the specification of a function (linear, quadratic, etc.) to fit a model to all the data in a given sample.

Coefficients of determination (R2) and Akaike's information criteria (AIC) were calculated for each model and reported to show the goodness of fit.

The "dynamic range" was determined for each parameter by subtracting the calculated measurement floor from the mean values in the healthy group. The relative values, defined as percentage of normal value, also were calculated. Knowing the test-retest variability of OCTA and SDOCT parameters allowed the determination of the average number of steps between mean healthy cpCD, pfVD, cpRNFL, and GCC thickness, measurements and their corresponding measurement floors. The number of steps to the floor was determined by dividing the dynamic range by the tolerance limit of inter-visit measurements in glaucoma patients. In this study, tolerance limits were chosen from previous reports as follows: **4.1** %

for cpCD19 using AngioVue, **4.4** % for pfVD19 using AngioVue, 4.95 μm for cpRNFL31 using Spectralis, and 3.1 μm for GCC4 using Optovue.

Results

Three hundred and thirty-two eyes of 198 glaucoma patients, 109 eyes of 63 glaucoma suspects and 68 eyes of 38 healthy individuals were included in this study.

Demographic and baseline ocular characteristics are presented in Table 1. VF MD ranged from −30.1 dB to 2.8 dB among all the eyes included in this study. The glaucoma group was composed of fewer females than males compared to the glaucoma suspect and healthy groups ($P = 0.003$). In addition, glaucoma eyes had thinner corneas ($P = 0.009$), worse mean baseline VF MD ($P < 0.001$), and greater VF PSD ($P < 0.001$) than glaucoma suspect and healthy eyes. The glaucoma suspect group had the highest IOP among the groups followed by healthy eyes and glaucoma eyes ($P = 0.002$). There were no significant differences among the groups in terms of age, race, systolic or diastolic blood pressure, MOPP, or axial length.

CpCD values were lowest in glaucoma eyes (42.2% [95% CI:41.4, 43.0]), followed by glaucoma suspect eyes (46.8% [95% CI: 45.6, 48.0]) and healthy eyes (50.2% [95% CI:49.3, 51.0]); all pairwise comparisons were statistically significant (Tukey's HSD, $P < 0.05$ for all comparisons). Similarly, pfVD values were lowest in glaucoma eyes (45.0% [95% CI: 44.4, 45.7]) followed by glaucoma suspect eyes (48.1% [95% CI: 47.3, 49.0]), and healthy eyes (50.0% [95% CI: 49.2, 50.7] (Tukey's HSD, $P < 0.05$ for all comparisons). Statistically significant differences also were found between healthy, glaucoma suspect and glaucoma eyes for cpRNFL and GCC thickness ($P < 0.001$).

The associations between cpCD, pfVD, cpRNFL thickness, GCC thickness, and VF MD along with LOWESS curves, coefficients of determination (R^2) and Akaike information criterion (AIC) using CPM and LOWESS are plotted in Figure 1. The LOWESS curve fitting the present data was similar to the predicted curve according to CPM indicated by similar AIC results describing goodness of fit.

The slopes of vessel density or thickness change before ($\beta + \alpha$) and after (α) the change points were evaluated using the CPM method (Table 2). A true floor was detected for cpRNFL thickness only. In another word, although cpRNFL thickness decreased after reaching the change point, the post-change point slope (α) was not significantly different from zero suggesting little thinning past this point. In contrast, cpCD and GCC thickness continued to decrease after their associated change points as disease severity increased. Although the differences between the pre-and post-change point slopes were statistically significant for cpVD, cpRNFL thickness and GCC thickness cpCD ($p<0.001$), no true change point was found for pfVD. This suggests that macular vessel density continues to decrease with increased disease severity represented in the current sample. The change point for GCC was identified earlier in the disease (MD = −7.2±1.1 dB) than for other variables (Table 2, Figure 1).

Estimating the Measurement Floors

No measurement floor was calculated for pfVD as a change point was not identified for this parameter using CPM. The post-CPM estimate of the measurement floor was 31.2 ± 1.1 % for cpCD, 49.5 ± 2.6 μm for cpRNFL thickness and 70.7 ± 1.0 μm for GCC thickness.(Table 3) No measurement floor was found for pfVD as a change point was not identified for this parameter using CPM. The estimate of the measurement floor was 31.2 ± 1.1 % for cpCD, 49.5 ± 2.6 μm for cpRNFL thickness and 70.7 ± 1.0 μm for GCC thickness.(Table 3) Corresponding VF MD at each estimated measurement floor was −19.3 ± 2.4 dB, −17.5 ± 3.3 dB and −13.9 ± 1.8 dB, respectively for each parameter, with GCC thickness reaching the estimated measurement floor at an earlier (i.e less severe) VF MD compared to cpRNFL and cpCD ($P<0.001$ for both comparisons.

Comparable results were found when the CPM model was adjusted for possible confounding variables (age, gender, quality index, and CCT). Specifically, no change point was identified for pfVD, and pfVD reached an estimated floor in the most advanced disease (VF MD: −25.80 ± 3.8 dB) followed by cpCD (VF MD: −19.7 ± 5.1dB), cpRNFL (VF MD: −16.5 ± 5·9 dB) , and GCC (VF MD: −14.3 ± 6.3 dB) ($P<0.05$ for all pairwise comparison except between cpCD and cpRNFL, $p=0.440$) (Table 4 , available at www.aaojournal.org). It should be noted that the LOWESS analyses did not adjust for covariates

Estimating the Dynamic Ranges

Table 3 also shows the dynamic range, relative dynamic range (percentage of normal value at the measurement floor), and number of steps from normal value to the estimated floor for each parameter. Because calculating dynamic range and the number of available steps requires a measurement floor and because CPM analysis did not identify a floor for pfVD, an arbitrarily defined floor was estimated using the mean values of all eyes with VF MD of −25.0 dB or worse.

The calculated dynamic ranges using CPM were 18.8% for cpCD, 43.9 μm for cpRNFL thickness and 22.8 μm for GCC thickness. The dynamic range was 16.7% for pfVD using the mean values of eyes with MD of −25.0 dB or worse. The relative dynamic range was greatest for cpRNFL thickness (47.0%), followed by cpCD (37.6%), pfVD (33.4%) and GCC thickness (24.4%). The number of steps from mean normal values to the floor was 8.9 for cpRNFL thickness followed by 7.4 for GCC thickness and 4.5 for cpCD. PfVD had the least number of steps from the normal value to the floor (3.8).

Discussion

The current results suggest that OCTA-measured macular vessel density was the least likely parameter to reach a measurement floor. This suggests that in late-stage glaucoma, particularly when VF MD is worse than −14 dB, OCTA-measured pfVD is a promising tool for monitoring progression. Although GCC and cpRNFL thicknesses reached their respective floors earlier along the glaucoma continuum, use of thickness parameters to detect glaucomatous progression may be advantageous within their dynamic range as they have more steps than OCTA parameters.

Optical coherence tomography angiography imaging provides a unique opportunity to measure vessel density of the retinal layer around the optic nerve and macula. OCTA vessel density measurements can detect glaucoma and reportedly have similar accuracy as cpRNFL in diagnosing glaucoma.[18, 20–24] Associations between superficial retinal microvasculature in the macula and the severity of visual field damage also have been reported.[6, 2023]

Based on the simple linear model, a change point was not found for pfVD in the current study. This indicates that this parameter does not reach a measurement floor until glaucoma is more severe (defined as a worse VF MD) than that observed in our sample, if at all. RNFL and GCC thickness reached their post-CPM estimated floors at an earlier stage of glaucoma than OCTA parameters. Although the slope of the cpCD curve decreased significantly after a VF MD of −13 dB (i.e. a change point was identified), it remained significantly different from zero, and thus did not reach a true measurement floor. In our model, cpCD reached the post-CPM estimated floor beyond −19.5 dB which was a lower VF MD than that estimated for both cpRNFL thickness and GCC thickness but a better VF MD than that estimated for pfVD.

Recently, Rao et al. examined vessel density-function relationships of peripapillary vessel densities in 227 eyes of 143 subjects and showed similar results in patients of East Indian ancestry.[32] Using linear and fractional polynomial models, they showed that optic nerve vessel density reached a measurement floor at a VF MD of approximately −15 dB. However, their population included fewer advanced glaucoma eyes than the current study. Moreover, they used an earlier OCTA algorithm that included large vessels along with capillaries in its estimation of vessel density. This might be of particular concern in advanced glaucoma eyes in which the large vessels might comprise a larger proportion of vessel density around the optic nerve than in earlier disease. By estimating the capillary density separately, we showed that cpCD was informative even in the later stage of the disease.

Similar to our study, several studies have reported structure-function relationships with cpRNFL thickness and VF in which cpRNFL thickness reached a measurement floor at a MD of −10 to −15 dB, beyond which little change in cpRNFL thickness was detectable.[9–12] Hood and associates measured cpRNFL thickness in 15 glaucoma eyes across a range of glaucoma severities using time domain OCT and tested the applicability of a previously described linear structure-function model; they found that cpRNFL thickness reaches an asymptotic floor at VF MD worse than −10 dB.[9, 10] Using a simple linear regression method, Mwanza and associates estimated that global cpRNFL change points obtained from Spectralis and RTVue were −14 dB and −10 dB, respectively.[12]

Recently, Belghith et al. detected significant change in GCIPL thickness in 31% of eyes with advanced glaucoma compared to 11% significant change in RNFL thickness.[14] Likewise, Shin et al.[15] demonstrated that OCT Guided Progression Analysis showed robust performance in the detection of progressive GCIPL thinning regardless of glaucoma severity. In contrast, RNFL GPA failed to detect progressive RNFL thinning in moderate to advanced glaucoma.[15] These results suggest that macular measurements may be superior to circumpapillary measurements for detecting change in moderate to advanced glaucoma. Although the change point for GCC thickness was calculated in relatively early disease

using CPM (VF MD = −7 dB) in the current study, we found weak but significant GCC thinning when MD was worse than −7 dB.

The estimated floors in the current study were 31.2% for cpCD, 33.4% for pfVD, 49.5 μm for cpRNFL thickness and 70.7μm for GCC thickness, which correspond to 60%, 66%, 53%, and 75%, of measurements in healthy subjects, respectively. The estimated floors for thickness parameters were similar to those previously reported in cross-sectional or longitudinal studies[9–12, 33–36] Previous cross-sectional analyses of different OCT instruments reported an estimated average RNFL thickness floor of 44.9 to 53.7 μm.[9–12,33–36] In other studies, the macular GCC residual thickness was calculated from 55 to 70 μm (68% to 73 % of normal value).[33–36]

Another useful clinical parameter that is complementary to the dynamic range of a parameter is the number of measurable steps from a normal value to the residual (i.e. floor) value. The number of steps represents another objective measure of monitoring disease progression that combines the variability of the measurement with the dynamic range. The more steps, the greater clinical utility of the test.[12] Test-retest variability directly affects this value.[26] In the current study, the calculated number of measurable steps was lowest for pfVD followed by cpCD, GCC thickness, and cpRNFL thickness. This suggests that cpRNFL thickness may be the best of the investigated parameters for detecting change from healthy to the measurement floor. Because pfVD did not result in a calculated measurement floor until very advanced disease, the number of steps in advanced glaucoma eyes may be larger than that of the other measurements. Although vessel density has fewer steps between the mean normal value and the floor, it is not known whether it has fewer steps in advanced disease.

This study has some possible limitations. First, the conclusions of this study are based on cross-sectional data and it is possible that the large inter-individual variability of measurements could result in reduced performance of these parameters in longitudinal data. Second, OCTA-measured vessel density is a surrogate but not a true measure of blood flow. Specifically, this modality detects vasculature based on amplitude decorrelation from perfused vessels but does not directly quantify the flow rate within the detected vessels. Moreover, the number of usable steps to the floor measurements is a function of test-retest variability, which may differ considerably across studies. For this reason, in addition to using the variability reported in Garas et al4 and Rao el[19] to estimate the number of steps, we also calculated the number of steps using the variability estimates reported by Manalastas et al[6] and found similar results for the number of steps in cpCD (4.9 steps) , pfVD (3.8 steps), and GCC (6.4 steps). Although the current study showed fewer number of steps for OCTA parameters, the test-retest variabilities of OCTA measurements that were used to calculate the number of steps were used estimates from prior OCTA software versions. It is possible that more recent software versions or OCTA instruments with higher resolution images will have better reproducibility which may result in more detectable steps in their dynamic range. Longitudinal studies are therefore needed to determine the usefulness of progressive vascular changes for monitoring advanced glaucoma using the newer higher density scans. Inclusion of some diabetic patients without retinopathy may have introduced a confounding effect on the results; there is some evidence that mild inner retinal thinning or microvascular

drop-out can be present before overt signs of diabetic retinopathy occur.[37, 38] However, the current comparisons among imaging methods that included eyes of diabetic patients with possible pre-diabetic retinopathy remain relevant because all methods were assessed using the same study population. Finally, our results may not be generalizable to other instruments with different scan resolutions and reproducibility characteristics.

In conclusion, the current study showed that OCTA-measured pfVD does not have a detectable measurement floor in late-stage glaucoma eyes. GCC and cpRNFL thicknesses reached their respective floors earlier along the glaucoma continuum. These results suggest that OCTA is a promising tool for detecting disease-related change in glaucomatous eyes in advanced disease. However, use of thickness parameters to detect glaucomatous progression are advantageous within their dynamic range as they have more steps than OCTA parameters. Longitudinal studies needed to identify the relative advantages of thickness versus OCTA parameters to detect progression in different stages of the disease.

Supplementary Material

Refer to Web version on PubMed Central for supplementary material.

Acknowledgements:

FUNDING/SUPPORT: Supported in part by National Institutes of Health/National Eye Institute grants R01 EY029058 (RNW), R21 EY027945 (CB), , EY011008 (LMZ), EY14267 (LMZ), and EY019869 (LMZ); by core grant P30EY022589; by an unrestricted grant from Research to Prevent Blindness (New York, NY); by grants for participants' glaucoma medications from Alcon, Allergan, Pfizer, Merck, and Santen, and by the donors of the National Glaucoma Research Program, a program of the BrightFocus Foundation.

Financial disclosures:

Linda M. Zangwill: Research support-Carl Zeiss Meditec, Heidelberg Engineering, National Eye Institute, Topcon, and Optovue; Robert N. Weinreb: Research support-Carl Zeiss Meditec, Centervue, Genentech, Heidelberg Engineering, Konan, National Eye Institute, Optos, Optovue, Tomey, and Topcon; Consultant-Aerie Pharmaceuticals, Allergan, Bausch & Lomb, Eyenovia, Novartis, Unity.

Abbreviations:

AIC	Akaike's information criterion
BP	blood pressure
CCT	central corneal thickness
CPM	change point model
cpRNFL	circumpapillary retinal nerve fiber layer
cpCD	circumpapillary capillary density
DIGS	Diagnostic Innovations in Glaucoma Study
GCC	ganglion cell complex
ILM	internal limiting membrane

IOP	intraocular pressure
IPL	inner plexiform layer
LOWESS	Locally weighted scatterplot smoothing
OCTA	optical coherence tomography angiography
ONH	optic nerve head
MD	mean deviation
MOPP	Mean ocular perfusion pressure
POAG	primary open angle glaucoma
pfVD	perifoveal vessel density
RGC	retinal ganglion cells
SDOCT	spectral domain optical coherence tomography
SSADA	split-spectrum amplitude-decorrelation angiography
SSI	signal strength index
VF	visual field

References:

1. Weinreb RN, Aung T, Medeiros FA. The pathophysiology and treatment of glaucoma: a review. JAMA 2014;311(18):1901–11. [PubMed: 24825645]
2. Weinreb RN, Khaw PT. Primary open-angle glaucoma. Lancet 2004;363(9422):1711–20. [PubMed: 15158634]
3. Traverso CE, Walt JG, Kelly SP, et al. Direct costs of glaucoma and severity of the disease: a multinational long term study of resource utilisation in Europe. Br J Ophthalmol 2005;89(10):1245–9. [PubMed: 16170109]
4. Garas A, Vargha P, Hollo G. Reproducibility of retinal nerve fiber layer and macular thickness measurement with the RTVue-100 optical coherence tomograph. Ophthalmology 2010;117(4):738–46. [PubMed: 20079538]
5. Mwanza JC, Chang RT, Budenz DL, et al. Reproducibility of peripapillary retinal nerve fiber layer thickness and optic nerve head parameters measured with cirrus HD-OCT in glaucomatous eyes. Invest Ophthalmol Vis Sci 2010;51(11):5724–30. [PubMed: 20574014]
6. Manalastas PIC, Zangwill LM, Saunders LJ, et al. Reproducibility of Optical Coherence Tomography Angiography Macular and Optic Nerve Head Vascular Density in Glaucoma and Healthy Eyes. J Glaucoma 2017;26(10):851–9. [PubMed: 28858159]
7. Bowd C, Zangwill LM, Berry CC, et al. Detecting early glaucoma by assessment of retinal nerve fiber layer thickness and visual function. Invest Ophthalmol Vis Sci 2001;42(9):1993–2003. [PubMed: 11481263]
8. Leung CK, Liu S, Weinreb RN, et al. Evaluation of retinal nerve fiber layer progression in glaucoma a prospective analysis with neuroretinal rim and visual field progression. Ophthalmology 2011;118(8):1551–7. [PubMed: 21529958]
9. Hood DC, Anderson SC, Wall M, Kardon RH. Structure versus function in glaucoma: an application of a linear model. Invest Ophthalmol Vis Sci 2007;48(8):3662–8. [PubMed: 17652736]

10. Hood DC, Kardon RH. A framework for comparing structural and functional measures of glaucomatous damage. Prog Retin Eye Res 2007;26(6):688–710. [PubMed: 17889587]
11. Mwanza JC, Budenz DL, Warren JL, et al. Retinal nerve fibre layer thickness floor and corresponding functional loss in glaucoma. Br J Ophthalmol 2015;99(6):732–7. [PubMed: 25492547]
12. Mwanza JC, Kim HY, Budenz DL, et al. Residual and Dynamic Range of Retinal Nerve Fiber Layer Thickness in Glaucoma: Comparison of Three OCT Platforms. Invest Ophthalmol Vis Sci 2015;56(11):6344–51. [PubMed: 26436887]
13. Bowd C, Zangwill LM, Weinreb RN, et al. Estimating Optical Coherence Tomography Structural Measurement Floors to Improve Detection of Progression in Advanced Glaucoma. Am J Ophthalmol 2017;175:37–44. [PubMed: 27914978]
14. Belghith A, Medeiros FA, Bowd C, et al. Structural Change Can Be Detected in Advanced-Glaucoma Eyes. Invest Ophthalmol Vis Sci 2016;57(9):OCT511–8. [PubMed: 27454660]
15. Shin JW, Sung KR, Lee GC, et al. Ganglion Cell-Inner Plexiform Layer Change Detected by Optical Coherence Tomography Indicates Progression in Advanced Glaucoma. Ophthalmology 2017;124(10):1466–74. [PubMed: 28549518]
16. Jia Y, Tan O, Tokayer J, et al. Split-spectrum amplitude-decorrelation angiography with optical coherence tomography. Opt Express 2012;20(4):4710–25. [PubMed: 22418228]
17. Weinreb RN. Ocular blood flow in glaucoma. Can J Ophthalmol 2008;43(3):281–3. [PubMed: 18504463]
18. Yarmohammadi A, Zangwill LM, Diniz-Filho A, et al. Peripapillary and Macular Vessel Density in Patients with Glaucoma and Single-Hemifield Visual Field Defect. Ophthalmology 2017;124(5): 709–19. [PubMed: 28196732]
19. Venugopal JP, Rao HL, Weinreb RN, et al. Repeatability of vessel density measurements of optical coherence tomography angiography in normal and glaucoma eyes. Br J Ophthalmol 2017.
20. Chen HS, Liu CH, Wu WC, et al. Optical Coherence Tomography Angiography of the Superficial Microvasculature in the Macular and Peripapillary Areas in Glaucomatous and Healthy Eyes. Invest Ophthalmol Vis Sci 2017;58(9):3637–45. [PubMed: 28728171]
21. Rao HL, Pradhan ZS, Weinreb RN, et al. Regional Comparisons of Optical Coherence Tomography Angiography Vessel Density in Primary Open-Angle Glaucoma. Am J Ophthalmol 2016;171:75–83. [PubMed: 27590118]
22. Rao HL, Pradhan ZS, Weinreb RN, et al. A comparison of the diagnostic ability of vessel density and structural measurements of optical coherence tomography in primary open angle glaucoma. PLoS One 2017;12(3):e0173930. [PubMed: 28288185]
23. Yarmohammadi A, Zangwill LM, Diniz-Filho A, et al. Optical Coherence Tomography Angiography Vessel Density in Healthy, Glaucoma Suspect, and Glaucoma Eyes. Invest Ophthalmol Vis Sci 2016;57(9):OCT451–9. [PubMed: 27409505]
24. Yarmohammadi A, Zangwill LM, Diniz-Filho A, et al. Relationship between Optical Coherence Tomography Angiography Vessel Density and Severity of Visual Field Loss in Glaucoma. Ophthalmology 2016;123(12):2498–508. [PubMed: 27726964]
25. Shoji T, Zangwill LM, Akagi T, et al. Progressive Macula Vessel Density Loss in Primary Open-Angle Glaucoma: A Longitudinal Study. Am J Ophthalmol 2017;182:107–17. [PubMed: 28734815]
26. Miki A, Endo T, Morimoto T, et al. Retinal nerve fiber layer and ganglion cell complex thicknesses measured with spectral-domain optical coherence tomography in eyes with no light perception due to nonglaucomatous optic neuropathy. Jpn J Ophthalmol 2015;59(4):230–5. [PubMed: 25963074]
27. Sample PA, Girkin CA, Zangwill LM, et al. The African Descent and Glaucoma Evaluation Study (ADAGES): design and baseline data. Arch Ophthalmol 2009;127(9):1136–45. [PubMed: 19752422]
28. Reis AS, O'Leary N, Yang H, et al. INFLuence of clinically invisible, but optical coherence tomography detected, optic disc margin anatomy on neuroretinal rim evaluation. Invest Ophthalmol Vis Sci 2012;53(4):1852–60. [PubMed: 22410561]
29. Wollstein G, Kagemann L, Bilonick RA, et al. Retinal nerve fibre layer and visual function loss in glaucoma: the tipping point. Br J Ophthalmol 2012;96(1):47–52. [PubMed: 21478200]

30. Cleveland WS, Devlin SJ. Locally Weighted Regression - an Approach to Regression-Analysis by Local Fitting. Journal of the American Statistical Association 1988;83(403):596–610.

31. Tan BB, Natividad M, Chua KC, Yip LW. Comparison of Retinal Nerve Fiber Layer Measurement Between 2 Spectral Domain OCT Instruments. Journal of Glaucoma 2012;21(4):266–73. [PubMed: 21637116]

32. Rao HL, Pradhan ZS, Weinreb RN, et al. Relationship of Optic Nerve Structure and Function to Peripapillary Vessel Density Measurements of Optical Coherence Tomography Angiography in Glaucoma. J Glaucoma 2017;26(6):548–54. [PubMed: 28333896]

33. Seong M, Sung KR, Choi EH, et al. Macular and peripapillary retinal nerve fiber layer measurements by spectral domain optical coherence tomography in normal-tension glaucoma. Invest Ophthalmol Vis Sci 2010;51(3):1446–52. [PubMed: 19834029]

34. Miraftabi A, Amini N, Morales E, et al. Macular SD-OCT Outcome Measures: Comparison of Local Structure-Function Relationships and Dynamic Range. Invest Ophthalmol Vis Sci 2016;57(11):4815–23. [PubMed: 27623336]

35. Kim NR, Lee ES, Seong GJ, et al. Structure-function relationship and diagnostic value of macular ganglion cell complex measurement using Fourier-domain OCT in glaucoma. Invest Ophthalmol Vis Sci 2010;51(9):4646–51. [PubMed: 20435603]

36. Rao HL, Qasim M, Hussain RS, et al. Structure-Function Relationship in Glaucoma Using Ganglion Cell-Inner Plexiform Layer Thickness Measurements. Invest Ophthalmol Vis Sci 2015;56(6):3883–8. [PubMed: 26070060]

37. Ng DS, Chiang PP, Tan G, et al. Retinal ganglion cell neuronal damage in diabetes and diabetic retinopathy. Clin Exp Ophthalmol 2016;44(4):243–50. [PubMed: 26872562]

38. Zeng Y, Cao D, Yu H, et al. Early retinal neurovascular impairment in patients with diabetes without clinically detectable retinopathy. Br J Ophthalmol 2019:bjophthalmol-2018–313582.

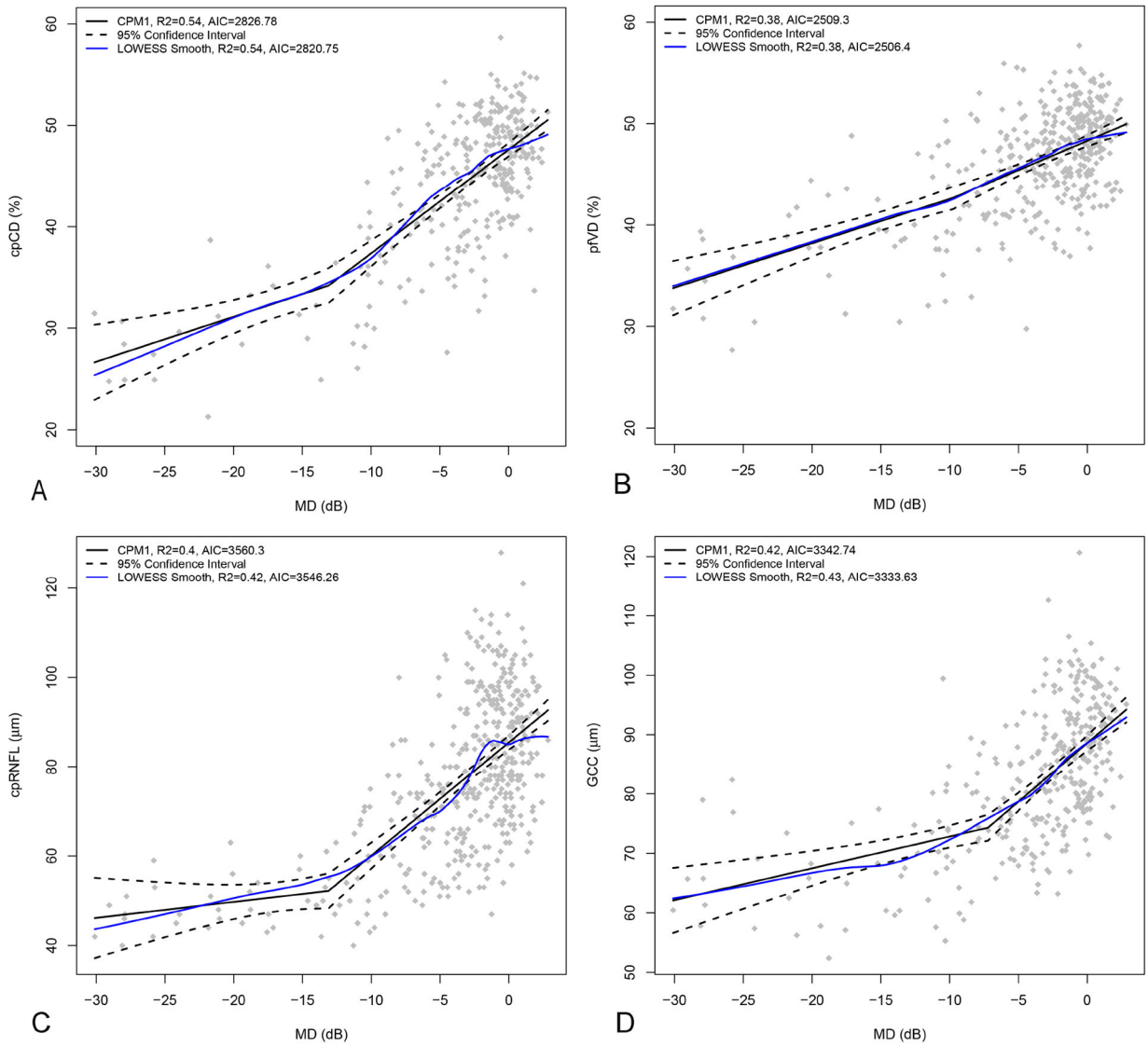

Figure 1.

Plot of change point analysis for vessel density-function relationship between circumpapillary vessel density (cpVD), perifoveal vessel density (pfVD) and visual field mean deviation (MD) (A, B) and thickness-function relationship between the circumpapillary retinal nerve fiber layer (cpRNFL) thickness, ganglion cell complex (GCC) thickness, and visual field MD (C, D).

The plain thick line represents the course of the predicted vessel density or thickness reduction as a function of visual field loss, the dotted lines are the upper and lower 95% confidence intervals and the solid blue line indicates the locally weighted scatterplot smoothing curve fitting the data. R2 represents the coefficient of determination. AIC: Akaike's information criterion.

Table 1.

Demographics and Ocular Characteristics of Study Population

	Healthy (95% CI)	Glaucoma suspect (95% CI)	Glaucoma (95% CI)	*P* value	Post Hoc
By subject (No.)	38	63	198		
Age (yrs.)	66.0 (63.9, 68.5)	68.7(66.0, 70.4)	69.1 (67.9, 70.2)	0.107	A=B=C
Gender (M/F)	9/29	23 /40	101/ 97	**0.003**	
Race, no. (%)				0.580	
Non−African American	31 (81.6%)	49 (77.8%)	147 (74.3%)		
African American	7 (18.4%)	14 (22.2%)	51 (25.7%)		
Self-reported history of Hypertension, n (%)	12 (31.5%)	37 (58.7%)	112 (56.5%)	**0.012**	
Diastolic BP (mmHg)	76.9(75.3, 80.6)	76.7 (76.1, 80.5)	78.1 (77.3, 79.7)	0.659	A=B=C
Systolic BP (mmHg)	129.9(124.9, 132.2)	128.3(126.2, 132.7)	128.7(126.5, 130.6)	0.906	A=B=C
By Eye (No.)	68	109	332		
MOPP(mmHg)	53.1(51.3, 54.9)	52.0(50.4, 53.7)	53.7(52.8, 54.7)	0.295	A=B=C
Axial Length (mm)	23.6 (23.3, 23.9)	24.1(23.9, 24.4)	24.2 (24.1, 24.4)	0.140	A=B=C
CCT (μm)	554.5(546.5, 562.6)	555.4(545.3, 565.6)	539.7(535.0, 544.5)	**0.009**	A=B>C
lOP(mmHg)	15.1(14.6, 15.7)	17.2(16.3, 18.1)	14.5(14.1, 15.1)	**0.002**	A=C<B
24-2 MD(dB)	0.1(−0.4, 0.2)	−1.12(−1.9, −0.3)	−5.6(−6.4, −5.0)	**<.0001**	A>B>C
24-2 PSD(dB)	1.7(1.6, 1.9)	2.3(1.9, 2.7)	5.6(5.3, 6.1)	**<.0001**	A<B<C
cpRNFL(μm)	93.4(90.2, 96.7)	85.4(82.6, 88.4)	71.7(69.9, 73.6)	**<.0001**	A>B>C
GCC(μm)	93.5(92.0, 95.1)	89.5(87.3, 91.7)	79.4(78.2, 80.8)	**<.0001**	A>B>C
pfVD (%)	50.0(49.2, 50.7)	48.1(47.3, 49.0)	45.0(44.4, 45.7)	**<.0001**	A>B>C
cpCD (%)	50.2(49.3, 51.0)	46.8(45.6, 48.0)	42.2(41.4, 43.0)	**<.0001**	A>B>C
Macula OCTA Quality Index	7.2 (7, 7.5)	6.9 (6.7, 7.2)	6.4 (6.2, 6.5)	**<.0001**	A=B>C
ONH OCTA Quality Index	7.3 (7.1, 7.5)	6.9 (6.7, 7.1)	6.7 (6.6, 6.9)	**0.001**	A>B=C

Categorical variables were compared using the chi-square test.

Other data were compared using linear mixed-model. Post hoc significance was using Tukey's honest significant difference test. Values with statistical significance are shown in bold.

Abbreviations: yrs, years; BP, blood pressure; cpCD: circumpapillary capillary density; MOPP, mean ocular perfusion pressure; MD, mean deviation; dB, decibels; OCTA: optical coherence tomography angiography; ONH: optic nerve head; pfVD: perifoveal superficial vessel density; PSD, pattern standard deviation; CCT, central corneal thickness.

Table 2.

Predicted slopes of steep and plateau lines, and change point sensitivity loss from change point model

	Slope (α) (95% CI)	*P Value*	Slope (β) (95% CI)	*P Value*	VF sensitivity at change point (dB)	*P Value*
cpRNFL	0.35 ± 0.46 (−0.55, 1.26)	0.441	2.18 ±0.50 (−0.55, 1.26)	**<.001**	−14.2 ± 1.3 (−16.9, −11.5)	**<.001**
GCC	0.47 ± 0.15 (0.16, 0.78)	**0.003**	1.71 ± 0.26 (1.19, 2.23)	**<.001**	−7.2± 1.1 (−9.4, −4.9)	**<.001**
pfVD	0.46 ± 0.08 (34.64, 38.45)	**<.001**	0.13 ± 0.11 (−0.10, 0.36)	0.271	−9.7 ± 8.0 (−25.6, 6.0)	0.226
cpCD	0.36 ± 0.66 (0.05, 37.42)	**0.021**	0.73 ± 0.17 (0.40, 1.07)	**<.001**	−13.0± 2.0 (−17.2, −8.9)	**<.001**

Abbreviations cpCD: circumpapillary capillary density; cpRNFL: circumpapillary retinal nerve fiber layer; GCC: ganglion cell layer; pfVD: perifoveal superficial vessel density.

α is the slope of the plateau portion in μm/dB or %/dB for thickness and vessel density, respectively.

β is the difference between the slope of the steep and plateau portions in μm/dB or %/dB for thickness and vessel density, respectively.

Table 3.

Structural and vasculature Residual Layers (floor), Their Corresponding Sensitivity Loss, Dynamic Range, relative dynamic range (percentage of normal value) and Number of Steps from Normal values to the Floor predicted by Post-Change Point Model

	Measurement floor*	VFMDat estimated floor, dB	Dynamic Range	Relative Range (%)	Number of Steps
cpRNFL(μm)	49.5 ± 2.6	− 17.5±3.3	43.9	47.0	8.9
GCC(μm)	70.7± 1.0	−13.9± 1.8	22.8	24.4	7.4
pfVD (%)	33.4± 2.7†	−25.8± 3.8	16.7	33.4	3.8
cpCD (%)	31.2+ 1.1	−19.3 ± 2.4	18.8	37.6	4.5

Abbreviations: cpCD: circumpapillary capillary density; cpRNFL: circumpapillary retinal nerve fiber layer; GCC: ganglion cell layer; MD: Visual Field; pfVD: perifoveal superficial vessel density.

* * 36, 96, 11, and 32 points were used to obtain the post-change point floor, for cpRNFL, GCC, pfVD, and cpCD, respectively.

† Calculated by averaging the values of eyes with MD of −25.0 dB or worse.